Journal of Environmental Management 156 (2015) 158–166

Contents lists available at ScienceDirect

Journal of Environmental Management

journal homepage: www.elsevier.com/locate/jenvman

Dissolved organic matter removal during coal slag additive soil aquifer treatment for secondary effluent recharging: Contribution of aerobic biodegradation

Liangliang Wei [a, b], Siliang Li [a, **], Daniel R. Noguera [b], Kena Qin [a], Junqiu Jiang [a], Qingliang Zhao [a, c, *], Xiangjuan Kong [d], Fuyi Cui [a, c]

[a] School of Municipal & Environmental Engineering, Harbin Institute of Technology, Harbin 150090, China
[b] Department of Civil and Environmental Engineering, University of Wisconsin-Madison, Madison, WI 53706, USA
[c] State Key Laboratory of Urban Water Resources and Environment (SKLUWRE), Harbin Institute of Technology, Harbin 150090, China
[d] Center of Science & Technology of Construction of the Ministry of Housing and Urban Rural Development, China

ARTICLE INFO

Article history:
Received 29 December 2014
Received in revised form
26 March 2015
Accepted 28 March 2015
Available online 2 April 2015

Keywords:
Soil aquifer treatment (SAT)
Coal slag
Dissolved organic matter (DOM)
Fractionation
Azide-inhibition

ABSTRACT

Recycling wastewater treatment plant (WWTP) effluent at low cost via the soil aquifer treatment (SAT), which has been considered as a renewable approach in regenerating potable and non-potable water, is welcome in arid and semi-arid regions throughout the world. In this study, the effect of a coal slag additive on the bulk removal of the dissolved organic matter (DOM) in WWTP effluent during SAT operation was explored via the matrix configurations of both coal slag layer and natural soil layer. Azide inhibition and XAD-resins fractionation experiments indicated that the appropriate configuration designing of an upper soil layer (25 cm) and a mixture of soil/coal slag underneath would enhance the removal efficiency of adsorption and anaerobic biodegradation to the same level as that of aerobic biodegradation (31.7% vs 32.2%), while it was only 29.4% compared with the aerobic biodegradation during traditional 50 cm soil column operation. The added coal slag would preferentially adsorb the hydrophobic DOM, and those adsorbed organics could be partially biodegraded by the biomass within the SAT systems. Compared with the relatively lower dissolved organic carbon (DOC), ultraviolet light adsorption at 254 nm (UV-254) and trihalomethane formation potential (THMFP) removal rate of the original soil column (42.0%, 32.9%, and 28.0%, respectively), SSL2 and SSL4 columns would enhance the bulk removal efficiency to more than 60%. Moreover, a coal slag additive in the SAT columns could decline the aromatic components (fulvic-like organics and tryptophan-like proteins) significantly.

1. Introduction

Water shortage and controlling wastewater pollution are two serious environmental issues in the arid and semi-arid regions (Bakopoulou et al., 2011; Dawadi and Ahmad, 2013). In addition, efficient reuse of secondary effluent from wastewater treatment plants (WWTP) is rapidly becoming a necessity for many municipalities (Wei et al., 2009a; Zhang et al., 2010). Because of its relatively easy operation, low constructional/operational cost, and high efficiency, soil aquifer treatment (SAT) has recently been employed to treat WWTP effluents via artificial water recharging, during which water quality is improved via the integrated functions of biochemical and physical processes (Nijhawan et al., 2013; Hubner et al., 2014). Reclaimed water from the SAT could be recycled for potable and non-potable uses after simple disinfection. Because there is strong evidence of the correlation between carcinogenic disinfection by-product (DBP) formation potential and the existence of dissolved organic matter (DOM) within the reclaimed water (Xue et al., 2008; Verlicchi et al., 2009), the search for new and innovative operation of SAT have focused attention on the environmental behavior and transformation of DOM.

DOM in the WWTP effluent is a heterogeneous mixture of organics, which consist of high-molecular-weight humic substances, polysaccharides, hydrophilic acids, aromatic proteins, and amino acids (Xue et al., 2008). DOM plays an important role in SAT

* Corresponding author. State Key Laboratory of Urban Water Resources and Environment (SKLUWRE), Harbin Institute of Technology, Harbin 150090, China.
** Corresponding author.
E-mail addresses: weill333@163.com (S. Li), zhql1962@163.com (Q. Zhao).

http://dx.doi.org/10.1016/j.jenvman.2015.03.049
0301-4797/

reclaimed systems, such as metals mobilization, pollutant degradation, and carbon release and utilization; moreover, it was also the main precursor of DBPs during chlorination of the reclaimed water (Sobhani et al., 2012). Biodegradation and adsorption processes are both contributors to DOM reduction during SAT operation (Fox et al., 2005), with biodegradation being dominant during traditional SAT operation. Being aware of the above described limitations, enhanced adsorption with activated carbon has been widely used in SAT operations (Schreiber et al., 2005; Acero et al., 2010). Taking environmentally acceptable and economical elements into consideration, cheaper adsorbents, such as red mud, fly ash, carbon slurry, peat, coal slag, and activated rice husks, have been attempted as substitutes of activated carbon (Cha et al., 2006; Gupta and Suhas, 2009; Wei et al., 2010; Geyikci et al., 2012). Because of its adsorptive characteristics and local availability (annual production of coal slag in China is estimated at approximately 0.5 billion tons), coal slag has been recently recognized as an alternative to granular activated carbon (GAC) (Dimitrova, 2002).

Coal slag and its modified products exhibited adsorptive properties and have been widely used in various industrial and sewage wastewater treatments for replacing currently used GAC (Liu et al., 2010; Li et al., 2011), and adsorption of dye, nickel, phosphorus, and lead are examples of coal slag use (Ortiz et al., 2001). A recent study by Genc and Oguz (2010) revealed that the removal efficiency of the dye Acid Yellow 99 could reach 50% at a slag dosage of 10 g/L, and its adsorption characteristics could be modeled with the Langmuir isotherm. In addition, physical and chemical surface modifications could enhance the dyes' adsorption efficiency (Xue et al., 2009b). Several studies have also shown that the adsorption of phosphorus by blast furnace slag follows a pseudo-second-order kinetic model (Kostura et al., 2005). Recently, an active melter slag filter was established in New Zealand to treat the effluent from waste stabilization ponds (McDowell et al., 2007), and 54%–84% of the bulk phosphorus was adsorbed (Pratt et al., 2007). Liu et al. (2010) demonstrated that the removal efficiency of Pb^{2+} (100 mg/L) would reach 96% under 30 g/L slag dosage. Moreover, Cha et al. (2006) stated that the addition of a steel slag would sharply enhance the bulk removal of organics during SAT treatment. Although the use of coal slag as a low cost adsorbent is increasing, few reports have been published on the application of coal slag modified SAT for secondary effluent recharging. In order to clarify the biodegradation removal mechanism of DOM during SAT operation, ultraviolet light (UV) and excitation-emission matrix (EEM) have been traditionally used for elucidating the biodegradability of dissolved organic carbon (DOC) (Azwa et al., 2013). To the authors' knowledge, no research has been performed to quantify the contribution of biodegradation and adsorption in coal slag additive SAT, which is essential for further studying the removal mechanism of DOM during SAT operation (McDowell et al., 2006; Xue et al., 2008).

The goal of work described here was to assess the contribution of a coal slag additive to the removal of DOM related trihalomethane (THM) precursors during SAT operation. The effect of coal slag modification on biomass activity, as well as the contribution of biodegradation and adsorption in DOM removal was also analyzed. Fluorescence spectrum analysis was applied to characterize the chemical structural variation of DOM fractions.

2. Materials and methods

2.1. Experimental materials

Experimental coal slag was collected from the boiler house of the Harbin Institute of Technology (Harbin, China). Prior to and in preparation for its use in the experiments, the coal slag was screened between 5 and 8 mm, washed and then dried at ambient temperature. The main composition of the coal slag was determined by X-ray fluorescence (XRF), resulting in a following chemical composition: 54.8–55.9% SiO_2, 22.4–27.2% Al_2O_3, 1.7–1.8% CaO, 0.5% MgO, 3.9–5.1% Fe_2O_3, 1.8–2.0% K_2O, 0.6% Na_2O, and 1.1–1.2% TiO_2 (w/w), with a loss on ignition (LOI) of 4.7–8.6%. An X-ray diffraction (XRD) spectrum showed abundant quartz (SiO_2), mullite ($Al_6Si_2O_{13}$), sodium aluminum phosphate ($Na_4Al_2Si_2O_9$), iron oxide (Fe_2O_3), and aluminum oxide (Al_2O_3). The density and Brunauer–Emmett–Teller (BET) specific surface of this coal slag as determined by standard methods was found to be approximately 2560–3320 kg/m^3 and 2.3 m^2/g (particular size of 120–250 mesh), respectively. Scanning electron microscope (SEM) images indicated a rugged and porous surface characteristic of the experimental coal slag (see Fig. S1, Supplementary material), which was observed by a MX2600FE scanning electron microscope (Camscan Company, U.K.).

Soil for the SAT columns packing was obtained from the dry riverbed of the Songhua River (Harbin, China) and further sieved to guarantee the diameter of soil particles being less than 2 mm. The packed soil samples had an average pH value of 8.1, organic carbon content (OC) of 3.1%, and cation exchange capacity (CEC) of 7.5 cmol/kg. The results of the particle size measurement indicated that the composition of the soil was 48.5% sand, 45.1% silt, and 6.4% clay, respectively. A XRF analysis indicated that the soil samples contained SiO_2 (61.5%), Al_2O_3 (16.4%), Fe_2O_3 (4.8%), K_2O (2.8%), MgO (1.7%), Na_2O (1.5%), CaO (1.3%), TiO_2 (0.7%), and LOI (8.2%).

Secondary effluent was obtained from the Taiping WWTP, Harbin (China), which has a design capacity of 3.25×10^5 m^3/d. Collection of secondary effluent was performed at least once a month between February 2011 and August 2012. The secondary effluent had a pH value of 7.8 ± 0.1, chemical oxygen demand (COD) of 13.7 ± 2.3 mg/L, DOC of 11.4 ± 1.5 mg/L, ultraviolet light adsorption at 254 nm (UV-254) of 19.3 ± 2.4 m^{-1}, suspended solids (SS) of 11.2 ± 6.2 mg/L, ammonia of 7.7 ± 1.9 mg N/L, and total phosphorus of 3.4 ± 1.3 mg/L.

2.2. Equipment and methods

XRD patterns of the experimental coal slag were collected with a Rigaku 2400 diffractometer (DMAX-2400, Rigaku, Japan) using Cu Kα (λ = 1.5406 Å) at step scan of 0.02° from 10° to 80°. The applied current and accelerating voltage were 20 mA and 40 kV. BET specific surface area of the coal slag was obtained using a Shimadzu 2360 micrometrics automatic surface area analyzer (Japan). The pH of water solutions and soil samples was measured using a pHS-3TC pH meter (Rex, Shanghai Precision Scientific Instrument Co., China). Electrical conductivity (EC) was determined from suspension with a 1:1 soil: water ratio according to USEPA Method 9050 using conductivity meter (DDS-11A, Shanghai Hongyi Instrument Factory). CEC was measured according to the USEPA Method 9081, by mixing soil with excess sodium acetate solution, and the concentration of displaced sodium was determined by atomic absorption emission spectroscopy.

DOC, UV-254 and EEM spectra of the DOM and its fractions were measured by a TOC-5000 Total Organic Carbon Analyzer (Shimadzu, Japan), a UV-2550 UV/VIS spectrophotometer (Shimadzu, Japan) and a Jasco FP-6500 spectrofluorometer (Tokyo, Japan), respectively. Specifically, each water sample was diluted to 1 mg/L of DOC with 0.01 mol/L KCl before EEM measurement, and was further acidified to pH 3 with HCl. The EEM spectra were obtained by scanning the sample over excitation wavelengths from 220 to 400 nm with 5 nm steps and emission wavelengths from 280 to 480 nm with 1 nm steps. A detailed description of these detection methods can be found in our previous studies (Xue et al., 2008; Wei et al., 2009b).

2.3. SAT column set-up

As shown in Fig. S2 (see Supplementary material), five 50 cm depth lab-scale SAT (diameter 10 cm) in parallel were constructed and packed with different materials, of which the SO column was packed with soil as a blank, and SSL1 and SSL2 columns were filled with a mixture of 75% soil/25% coal slag (v/v) and 50% soil/50% coal slag (v/v), respectively. Specifically, the sieved coal slag and soil were mixed homogeneously, then packed into the columns and further compacted to field density, the average density of the coal slag/soil mixture was 2883 kg/m^3 for SSL1 and 2431 kg/m^3 for SSL2, respectively. To assess the corresponding effect of the packed coal slag on biodegradation, the top 25 cm layer of the SSL3 and SSL4 was filled with soil, whereas the lower layer of 25 cm was packed with a mixture of 75% soil/25% coal slag (v/v) for SSL3 and 50% soil/50% coal slag (v/v) for SSL4. All five SAT columns were operated with a cycle of 16-h wetting to 8-h drying under a constant temperature of 25 ± 2 °C (Xue et al., 2009a), and the secondary effluent was pumped through the columns at a flow rate of 15 mL/h.

To investigate the effect of coal slag addition on microbial activity, the experimental secondary effluent was spiked with 2.0 mmol/L sodium azide (NaN_3) to inhibit aerobic biodegradation, and then introduced to another five columns which were filled as described above. The two systems were operated for almost six months.

2.4. Fractionation procedure

After six months of operation, the effluent DOM of the inhibited and uninhibited SAT columns was fractionated using Amberlite XAD-8/XAD-4 resins into five fractions: hydrophobic acid (HPO-A), transphilic acid (TPI-A), hydrophobic neutral (HPO-N), transphilic neutral (TPI-N) and hydrophilic fraction (HPI). The detailed description of the methods was given in our previous study (Xue et al., 2008). All fractionated organic samples were adjusted to a pH of 7.0 ± 0.1.

2.5. Speciation analyzing of heavy metals in coal slag

The experimental coal slag was digested using an acid mixture (HCl:HNO_3:HF) ratio of 3:3:2 in a microwave oven, then the concentrations of toxic heavy metals were determined by inductively coupled plasma mass spectrometry (ICP-MS). Moreover, sequential extraction experiment was also employed to provide information on the chemical distribution of heavy metals in coal slag for risk assessment (Tessier et al., 1979). Samples were subjected to specific solvents in a five-step sequential extraction procedure; the modes of occurrences of trace elements were classified into five fractions: exchangeable, carbonate-bound, Fe–Mn oxides bound, organic matter bound, residual. The fractions acquired after each extraction step were analyzed for Cu, Mn, Zn, As, Pb and Cr by ICP-MS. Each of the samples was analyzed in duplicate.

2.6. Chemical analyses

Reactivity of DOM fractions towards chlorine and trihalomethane formation potential (THMFP) was assessed in terms of specific THMFP (STHMFP). Prior to chlorination, each of the freeze-dried DOM fractions was diluted with ultrapure water (Milli-Q water) to produce a DOC concentration of 1 mg/L, subsequently buffered with 0.05 mol/L phosphate solution. The chlorination was performed by adding adequate excess amount of concentrated sodium hypochlorite (5 mg–Cl_2/mg–C) into the buffered organic fractions for seven days under 25 ± 2 °C. Residual chlorine after reaction was immediately quenched with Na_2SO_3 and the analysis of the fractional THMFP was conducted without delay.

3. Results and discussion

3.1. DOC and UV-254 variations of the effluent obtained from five columns

Both DOC concentration (Fig. 1a) and UV-254 (Fig. 1b) of the SSL1-SSL4 effluents decreased gradually during the first 10 days of operation, while the SO effluent remained constant, ascribing to the leachate organic matter from the packed coal slag. In the subsequent steady-state study period (11–60 days), the average DOC removal efficiencies were SSL4 (64.9%) > SSL2 (63.9%) > SSL3 (50.8%) > SSL1 (48.7%) > SO (42.0%) (Fig. 1a). The SSL2 column showed the highest UV-254 reduction (72.8%), followed by the SSL4 (58.4%), the SSL1 (49.2%), the SSL3 (40.4%), whereas that of the SO was the lowest (31.9%). The relatively higher DOC reduction in SSL2 than in SSL1 was correlated with the greater amount of coal slag in SSL2. In comparison to our previous study, which used fly ash as the supplementary material (Wei et al., 2010), the addition of the coal slag significantly enhanced the bulk DOM reduction during the SAT processing, especially for the aromatic organics reduction. In addition, the removal efficiency of the DOC in this study is higher than the traditional SAT column systems with a depth of 80 cm and 100 cm (Quanrud et al., 1996, 2003), and this efficiency was comparable to the findings of Westerhoff and Pinney (2000) and Xue et al. (2007; 2009a), who constructed 82 cm and 150 cm length soil columns, respectively. All of those results undoubtedly demonstrate that the addition of coal slag in SAT system is beneficial. A summary of some relevant published literature with the latest results on DOM removal in SAT systems is presented in Table 1, and some of these results have already been discussed here.

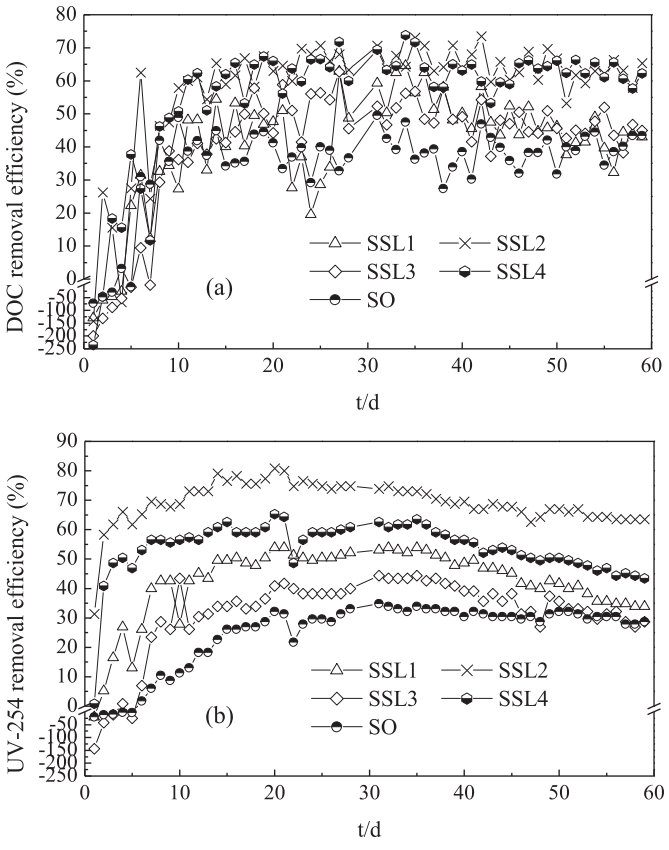

Fig. 1. DOC (a) and UV-254 concentration (b) of SSL1-SSL4 and SO column effluents.

3.2. Aerobic inhibition of different SAT columns and DOM removal

To characterize the biodegradable removal mechanism of DOC within the coal slag-added SAT systems, the operation of lab-scale azide-inhibited SAT columns and uninhibited SAT columns was compared. As shown in Table 2, as high as 42.0% of the DOC was removed by the uninhibited SO column, leading to a low effluent DOC of 6.52 mg/L. The DOC removal efficiency in the azide-inhibited SO column was averaged 13.9%, yielding an effluent concentration of 9.67 mg/L. As Xue et al. (2009a) reported, sodium azide inhibition would eliminate aerobic microbial activity, thus the DOC reduction in the sodium azide inhibited columns could be ascribed to a combination of sorption (soil and coal slag) and anaerobic biodegradation. The DOC removal efficiency of the uninhibited SO column was approximately 3.4 times as high as the inhibited columns, implying that aerobic degradation was the predominant mechanism for the reduction of DOC during SAT operation. In comparison with the uninhibited columns, the DOC removal efficiency of the four inhibited columns was significantly lower, showing a distribution trend of SSL1 (38.0%) < SSL2 (38.3%) < SSL4 (50.4%) < SSL3 (60.4%). It should be noted that a more significant decreasing of DOC removal efficiency of SSL3 and SSL4 in comparison with that of the SSL1-2 columns was ascribed to the inhibition of aerobic activity in the top soil layer, which played a dominating role in DOC reduction during the processing of those two columns. A similar UV-254 removal trend was observed between inhibited and uninhibited columns, the declining rate of UV-254 showed a decreasing trend of SSL1 (23.9%) < SSL2 (25.3%) < SSL3 (33.2%) < SSL4 (34.6%) < SO (53.5%) after azide-inhibition. It is noted that eliminating aerobic activity had a less negative effect on UV-254 precursor removal compared with the DOC, especially for the coal slag additive columns, due to the preferred adsorption of aromatic components by soil or coal slag (Bakopoulou et al., 2011).

In comparison with the uninhibited columns, the effluent SUVA value of the azide-inhibited SSL3, SSL4, and SO columns decreased 22.9%, 24.1%, and 17.0%, respectively, much higher than that of the azide-inhibited SSL1 and SSL2 columns. The main reason might be that the significant biodegradation of SSL3, SSL4 and SO could remove the non-aromatic components preferentially, leading to a significant increasing in SUVA. On the other hand, adsorption and anaerobic biodegradation in the SAT system would remove the aromatic macromolecules preferentially, and that might be the main reason for the low SUVA decreasing of azide-inhibited SSL1 and SSL2 columns.

3.3. Fractional DOC and UV-254 removal during different SAT column operations

HPI (40.7%) and HPO-A (29.8%) were the predominant organic fractions in secondary effluent, and the other three fractions were TPI-A (13.1%), HPO-N (9.9%), and TPI-N (6.5%). As illustrated in Fig. 2a, the removal efficiency of HPI during the columns processing decreased as SSL4 (61.6%) > SO (59.9%) > SSL3 (59.4%) > SSL2 (54.9%) > SSL1 (50.7%). However, the SSL1-2 systems showed a much higher DOC reduction of the hydrophobic fractions, and the DOC reduction of HPO-A and HPO-N were 76.8% and 70.7% during SSL2 processing. In comparison, only a 39.2% reduction of HPO-A and a 29.6% of HPO-N was observed for the SO column. Generally, HPO-A has the least electrical charge and the highest molecular weight among these DOM fractions, and HPI showed the highest biodegradability, whereas HPO-N, TPI-A and TPI-N had the intermediate chemical characteristic (Quanrud et al., 2004). The results above demonstrated that despite the packed coal slag affecting the biodegradation of HPI partially, it adsorbed the hydrophobic materials efficiently. For the TPI-A fraction, the SSL2 showed the highest DOC removal efficiency of 70.9% among all of the columns, followed by SSL4 (58.5%), SSL1 (50.5%) and SSL3 (45.1%), whereas only 30.6% for the SO column. A similar DOC removal trend was also found for the TPI-N as follows: SSL4 (72.0%) > SSL3 (59.1%) > SSL2 (54.9%) > SSL1 (47.3%) > SO (39.7%). It should be noted that SSL4 was efficient in removing the all five DOM fractions regardless of their hydrophobic/hydrophilic characteristics.

The average UV-254 removal rates of the SSL1, the SSL2, the SSL3, the SSL4, and the SO columns were 49.2%, 72.8%, 40.4%, 58.4%, and 32.9% during the steady process period, respectively (Fig. 2b). The SO led to the lowest UV-254 reduction of HPO-A and TPI-A (26.1% and 16.2%, respectively) among all five columns, whereas the SSL2 was the highest (79.8% and 69.7%, respectively). For comparison, a higher UV-254 reduction of HPI (55.0%) was obtained from the SO column, than that of the SSL4 column (51.2%), but lower than the SSL2 (67.7%). These results indicated that the hydrophobic aromatic DOM could be efficiently adsorbed by the packed coal slag, whereas the aromatic HPI could be readily biodegraded by the biomass within the top soil layer, was consistent with results in Table 2. Interestingly, a higher UV-254 removal of

Table 1
Overviews of DOC removal in artificial aquifer recharge systems.

Reference and authors	Influent DOC (mg/L)	Removal efficiency (%)	Column depth/Distance from recharging point (m)	Effluent DOC (mg/L)	Operational time	Other information
Quanrud et al., 1996	11	54	1.0	5.1	21 weeks	
Quanrud et al., 2003	13	56	0.8	5.7	5 years	
	13	75	1.5	3.3	5 years	
Amy and Drewes, 2007	14.1	66	6.0	4.8	11 months	
	14.1	93	35	1.0	11 months	
	6.1	76	388	1.5	6–18 months	
	6.1	71	655	1.8	6–18 months	
	6.1	75	885	1.5	6–18 months	
	6.1	82	2700	1.1	6–18 months	
Westerhoff and Pinney, 2000	12.6	66	0.82	4.3	10–35 weeks	2.8 mg OC/g soil
	13.6	39	0.82	8.3	10–35 weeks	4.5 mg OC/g soil
Drewes et al., 2003	5.64	77	2000	1.23	12–18 months	
Fox et al., 2005	10.4	37	2.0	6.8	500 days	
Cha et al., 2006	4.6	20	0.5	3.6	8 months	
Xue et al., 2007, 2009a	11.6	47	0.5	6.3	130 days	
	11.6	61	1.0	4.7	130 days	
	11.6	67	1.5	3.9	130 days	

Table 2
DOC, UV-254, and SUVA distributions of five different SAT columns which modified by coal slag under uninhibited condition and azide-inhibited condition.

Parameters			SSL1	SSL2	SSL3	SSL4	SO
DOC	Original column	Effluent (mg/L)	5.77	3.94	5.53	4.06	6.52
		Removal (%)	48.7	64.9	50.8	63.9	42
	NaN_3 inhibited column	Effluent (mg/L)	7.85	6.74	8.68	7.62	9.67
		Removal (%)	30.2	36.4	22.8	31.7	12.9
UV-254	Original column	Concentration (mg/L)	7.01	3.75	8.22	5.74	9.4
		Removal (%)	49.2	72.8	40.4	58.4	31.9
	NaN_3 inhibited column	Concentration (mg/L)	8.76	6.39	10.24	8.63	11.78
		Removal (%)	36.5	53.7	25.8	37.4	14.6
SUVA	Original column		1.26	1.03	1.53	1.49	1.47
	NaN_3 inhibited column		1.12	0.95	1.18	1.13	1.22

HPI from the SSL2 compared with that of the SO partially indicated biomass was formed within the coal slag. In addition, the UV-254 removal efficiencies from all five SAT columns were lower than the corresponding DOC removal efficiencies.

As shown in Fig. 2a, the effect of azide-inhibition on the removal of hydrophobic fractions was much lower than that of the hydrophilic fraction. Interestingly, the removal rate of HPI decreased significantly (ranged from 42.6% to 65.7%) during the five azide-inhibited columns compared with the uninhibited columns. However, the declining rate of the HPO-A removal efficiency was less than 40% for the coal slag additive columns, and the four columns decreased as SSL1 (18.9%) < SSL2 (26.2%) < SSL3 (38.7%) < SSL4 (39.8%), much less than that of the SO (55.9%). A similar removal trend was observed for the TPI-A fraction, implying less influence of azide-inhibition for acid organic removal during coal slag additive columns processing (declining rate of DOC removal efficiency less than 24.4% for SSL1-2). From above, we can conclude that the aerobic activity in the traditional SAT system played a major role, both for hydrophobic and hydrophilic fractions removal, especially for HPI fraction.

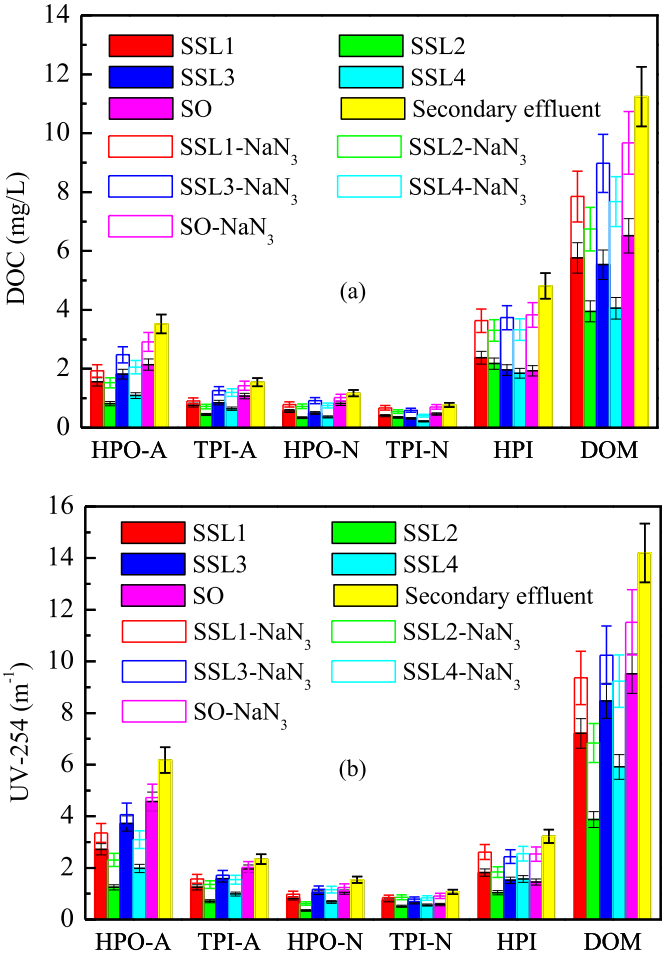

Fig. 2. Fractional DOC concentrations (a) and UV-254 (b) of SFA1-SFA4 and SO column effluents for the azide-inhibited and uninhibited SAT columns.

The transformation trend of aromatic materials in the secondary effluent during the five SAT columns (with vs. without azide-inhibition) operation was similar to that of DOC. The removal of HPO-A- and TPI-A-related aromatic materials during SO column operation was slightly influenced by the inhibition of aerobic biodegradation (decreased 9.8% and 15.9% compared with the traditional SAT), implying that the removal of those aromatic components was mainly attributed to the anaerobic biodegradation and adsorption in the soil. In addition, the UV-254 removal efficiency of HPO-A was decreased by 26.5% and 21.5% for the SSL4 and the SSL2 columns, indicating that those aromatic components adsorbed on coal slag could be partially aerobic and anaerobic biodegraded. The removal trend of UV-254 of TPI-A was similar to that of HPO-A, which decreased as SSL4 (41.2%) > SSL2 (39.5%) > SSL1 (29.6%) > SSL3 (17.1%) > SO (15.9%). However, the removal of aromatic components in HPI fraction was negatively affected by the azide-inhibition, and the declining rate of UV-254 removal efficiency of the SSL1, the SSL3, the SSL4, and the SO columns was more than 50%, indicating that aerobic biodegradation was the main reason for the removal of HPI related aromatic materials.

3.4. THM precursors removal by different SAT columns

HPO-A and HPI were the major THM precursors in the secondary effluent (245.0 μg/L for HPO-A vs. 157.4 μg/L for HPI), and TPI-A was another major THM precursor (64.2 μg/L). Generally, the effluent collected from SO exhibited the highest THMFP value (387.6 μg/L) in comparison with other four effluents, meanwhile its STHMFP value increased from 47.9 μg/mg to 59.5 μg/mg after the SAT processing, implying the 50 cm soil layer was less efficient in removal the THMs precursors (Fig. 3). Correspondingly, all of the columns with coal slag addition showed a higher THMFP reduction, ascribing to the preferential adsorbing of hydrophobic THM precursors by the coal slag. It should be noted that SSL2 performed better on THMFP removal (67.8%) and STHMFP reduction (8.3%), demonstrating a higher coal slag additive would adsorb more THMs precursors. On the other hand, a 44.7% removal of THMFP (STHMFP increased 12.3%) in the SSL3 effluent clarified that the configuration design of an upper 25 cm soil layer, with a relatively lower addition of coal slag mixture underneath, is less efficient on THMFP removal. In addition, up to a 60.9% reduction of THMFP was observed during the SSL4 process, with a significant increasing of STHMFP (8.5%),

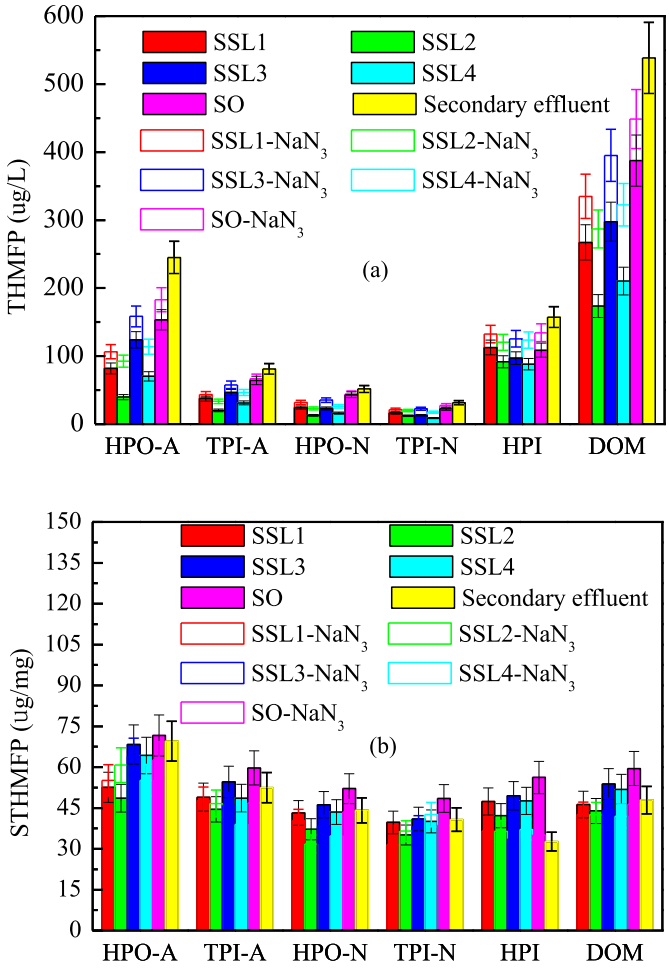

Fig. 3. Variation of THMFP (a) and STHMFP (b) of SFA1-SFA4 and SO column effluents for the azide-inhibited and uninhibited SAT columns.

implying efficient biodegradation within the top soil layer.

Coal slag in SAT columns enhanced the bulk reduction of the non-hydrophilic THM precursors. Ultimately, SSL1 would preferentially remove the THM precursors in acidic and hydrophobic fractions, whereas SSL4 and SSL2 would also remove the hydrophilic materials. Removal efficiency of THMFP in HPO-A during the five processes decreased as SSL2 (83.8%) > SSL4 (71.4%) > SSL1 (66.5%) > SSL3 (49.4%) > SO (37.4%). The results above clearly demonstrated that a higher ratio of the coal slag additive in the SAT system is essential for the removal of HPO-A-related THM precursors. The SSL4 column showed the highest THMFP reduction of 44.0% in HPI, followed by SSL2 (41.7%), SSL3 (38.4%), and SO (31.0%), whereas that of the SSL1 was the lowest (28.5%). The results above implied that the reserving of the upper 25 cm of the soil layer is meaningful for the removal of HPI-related THMs precursors, which always showed a lower molecular characteristic. The removal trend of the THMs precursors in the fractions of HPO-N and TPI-A was similarly to that of HPO-A.

STHMFP value of HPO-A was declined 24.4% and 30.1% during SSL1 and SSL2 column processing, respectively (Fig. 3b), and showed a much lower STHMFP than those of the other three effluents. STHMFP value of TPI-A, HPO-N and TPI-N were decreased about 15% during the SSL2 operation, but not significantly for other four effluents. Contrarily, STHMFP of HPI was substantially increased for all five columns. Despite HPI-related STHMFP of SSL4 effluent was increased by 45.8%, a relatively higher fractional DOC removal of SSL4 would also lead to a 60.9% reduction of THMFP. Thus, the reserving of the upper 25 cm soil layer was practically necessary for removal of hydrophilic THMs precursors for coal slag additive SAT system.

The THMFP of the SO column (average 448.5 μg/L), which was inhibited by azide, was much higher than that of the non-inhibited effluent, indicating the aerobic biodegradation played a major role in the THMs precursor removal. Aerobic inhibition showed a significant influence on SSL3 and SSL4 in THMFP removal, while that of the SSL1 and SSL2 was only slightly influenced (334.9 μg/L and 287.0 μg/L, respectively). Removal efficiency of the THM precursors in the HPI fraction during all five columns operations decreased significantly after the azide-inhibition (ranged from 43.4% to 52.5%). Compared with the HPI, the negative influence of the azide on the removal of the HPO-A-related THM precursors was less significant (ranged from 15.0% to 32.1%), which showed a decreased trend of SO > SSL3 > SSL2 > SSL4 > SSL1. The result above indicated that the traditional and coal slag additive SAT system, which had certain adsorption ability, was inclined to remove more hydrophobic aromatic THM precursors, especially under the inhibition of aerobic biodegradation. In addition, the STHMFP value of all five columns increased (ranged from 3.1% to 22.0%) after the aerobic inhibition, indicating the aerobic biodegradation was the main reason for removing non-THM precursors. This could be further proven by the more significant increasing of the STHMFP of HPI in comparison with that of the HPO-A fraction. Moreover, the declining rate of the STHMFP of the SSL1 and the SSL2 was less than that of the SSL3 and the SSL4 when the aerobic biodegradation was inhibited, implying that the adsorbed THM precursors on coal slag could be efficiently biodegraded by the biomass within the SAT system, especially for the hydrophobic fractions.

3.5. Fluorescence spectroscopic analysis

As shown in Fig. 4f, the EEM spectrum of the secondary effluent was dominated by humic-like (Ex/Em = 265–300/380–440 nm), tryptophan-like (Ex/Em = 220–260/280–332 nm and 220–260/332–380 nm), and fulvic-like fluorescence (Ex/Em = 240–260/380–480 nm), which also exhibited a shoulder of soluble microbial by-products (SMP) and aromatic protein peaks (Ex/Em = 260–300/332–380 nm) (Chen et al., 2003; Wei et al., 2009a). Once the coal slag additive slag had progressed, a significant SMP fluorophore was observed for the SSL1, the SSL3 and the SSL4 columns (similar to the SO column), whereas less significant for SSL2. The results above indicate that a higher quality additive of coal slag might partially affect the activity of the biomass, which is consistent with the observation of the azide-inhibition results. Compared with our previous study, the negative effect of the coal slag on the biomass in the SAT column is much less than that of the fly ash additive system (Wei et al., 2010).

Intensity order of the fulvic-like fluorophores (Ex/Em = 230–260/380–480 nm) with respect to the effluent of five non-inhibited columns was found to be SO > SSL3 > SSL1 > SSL2 > SSL4, indicating that both of the traditional SAT system and a low quality coal slag additive SAT (SSL3) were less efficient in removing the fulvic-like fluorophores. A sharp decline of intensity of the fulvic-like peak after the SSL2 processing was ascribed to the efficient adsorption of coal slag. On the other hand, the combination of the adsorption of the coal slag and the biodegradation in the upper 25 cm soil layer in SSL4 would lead to a lowest fluorescent intensity of the fulvic acid-like materials.

The effluent of the SSL1, SSL3, SSL4, and SO columns showed a noteworthy fluorophore of tryptophan-like proteins after the columns' operation, in which SO was the highest, indicating a lower quality additive of the coal slag or that the reserving of the upper 25 cm soil layer is meaningful for the well-function of the biomass

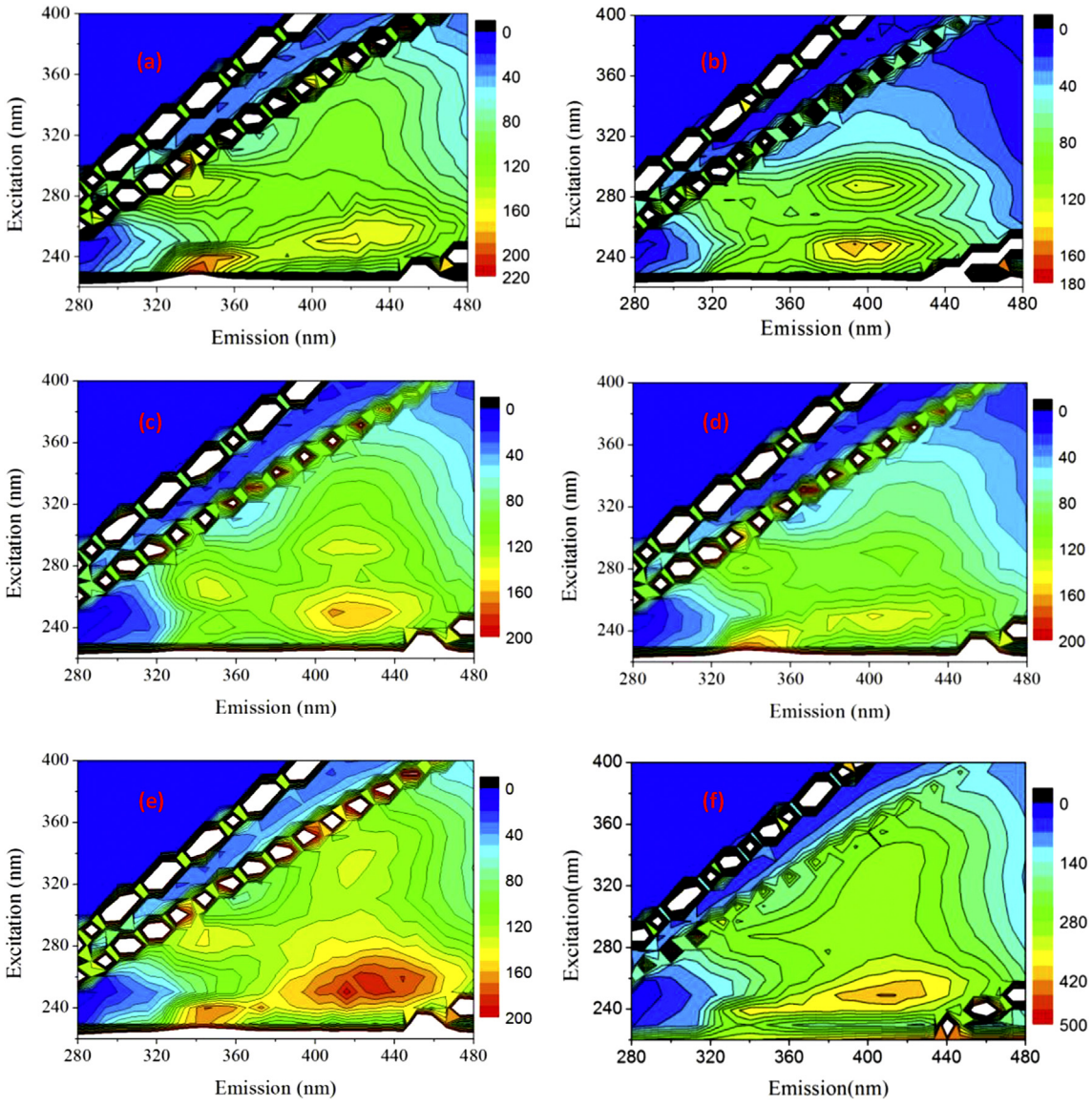

Fig. 4. Fluorescence EEMs for the column effluent of SSL1(a), SSL2(b), SSL3(c), SSL4(d), SO(e) and the secondary effluent (f).

within the coal slag additive columns, which could be further proven by the lowest intensity of the tryptophan-like proteins fluorophore of the SSL2 column. Moreover, the biodegradation in the SAT could lead to the formation of new tryptophan-like aromatic proteins.

The SSL2 column effluent showed a much higher fluorescent intensity of the humic-like groups compared with the other four columns, implying that reduction of humic-like fluorescence during SAT processing mainly resulted from biodegradation instead of adsorption. Bu et al. (2010) and Yang et al. (2008) demonstrated that the humic-like activated aromatic sites, especially the aromatic β-diketones, aromatic anthropogenic substances and the aromatic polyhydroxy moieties, were the main THMs precursors. As a result, a sharply intensity declining of the fluorescence peak at Ex/Em = 265–300/380–440 nm implied that the packed coal slag would efficiently adsorb those aromatic humic-like THMs precursors.

3.6. Ecological risk assessment

The presence of heavy metals in coal combustion products (slag and fly ash) is a concern due to their persistent toxicity and the potential ecological risk during the SAT operation (Zhou et al., 2013; Komnitsas et al., 2013), and the soil and groundwater were always considered as the environmental targets for the pollution (Tiruta-Barna et al., 2007). Generally, the risk of the heavy metals increased almost linearly with the exchangeable elements percentage (exchangeable and carbonate-bound heavy metals), hence, the risk assessment code was defined as the fraction of exchangeable elements in the total species distribution in the total species distribution (Nemati et al., 2011). When the percentage mobility was <1%, there has no risk to the environment. Correspondingly, percentage mobility of 1–10%, 11–30% and 31–50% indicated the level of low risk, medium risk and high risk, respectively.

The average concentration of Cu, Mn, Zn, As, Pb and Cr in the experimental coal slag was 5.3, 87.4, 53.6, 3.17, 6.79 and 17.6 mg/kg, respectively, and the speciation distribution of the exchangeable, carbonate-bound, Fe–Mn oxides bound, organics bound and residue heavy metal fractions of those six heavy metals is shown in Fig. S3 (see in Supplementary material). As shown in Fig. S3, the majority of the heavy metals remained in the residue fraction (ranged from 87.3% to 95.1%), indicating that the heavy metals in

the coal were efficiently stabilized and solidified during the incineration process (Rio et al., 2007; Lin et al., 2014). Specifically, the percentage mobility of the six heavy metals in coal slag showed a decreased trend of Cu (4.7%) > Zn (4.3%) > Pb (3.4%) > As (3.3%) > Mn (2.7%) and Cr (1.1%), indicating that all those six heavy metals presented a low leaching potential, and eventually declined the ecological risk of the application of coal slag SAT. The leaching experiments of Al, Ca, Cr and Pb during the five column operation (see in Table S1, Supplementary material) indicated that despite observing a slight increase of Al^{3+} and Ca^{2+} in columns with coal slag addition, no significant heavy metal (Cr and Pb) leaching was observed during the steady-state operation of the coal slag additive SAT system. Similar results were obtained by Abbott et al. (2003) and Francois (2001) for the using of municipal solid waste incineration bottom ashes as the sub-base of the road, they observed no significant leaching of heavy metals to the underneath soil layer.

4. Conclusions

Aerobic biodegradation accounted for 70.6% of the bulk DOM removal in traditional 50 cm SAT column operation. Coal slag addition significantly enhanced the adsorption of hydrophobic components in comparison with traditional SAT systems without coal slag. Furthermore, the hydrophobic DOM adsorbed on coal slag was found to be partially biodegraded aerobically. A higher reduction of hydrophobic components, along with a lower removal of hydrophilic materials, was observed within the coal slag-packed columns (especially for SSL1 and SSL2), in which the removal of the hydrophilic organics was mainly attributed to aerobic biodegradation. Thus, the configuration design of the upper 25 cm soil layer overlaid on the mixture of soil and coal slag was necessary. The coal slag addition lead to an efficient removal of the THM precursors, a decrease of the STHMFP, and exhibited a relatively low ecological risk of heavy metal leaching. In addition, the coal slag addition decreased the intensity of tryptophan-like aromatic proteins and humic-like components, while fulvic-like components showed a relatively high reduction during the SO column treatment.

Acknowledgments

The authors gratefully acknowledge funding from Project 51408159 supported by National Nature Science Foundation of China, the supports by State Key Laboratory of Urban Water Resource and Environment, Harbin Institute of Technology (No. 2013TS03), the China Postdoctoral Science Foundation funded projects (2013T60375 and 2012M520744), as well as the Project Supported by Natural Scientific Research Innovation Foundation of Harbin Institute of Technology (HIT.NSIRF.2013111).

Appendix A. Supplementary data

Supplementary data related to this article can be found at http://dx.doi.org/10.1016/j.jenvman.2015.03.049.

References

Abbott, J., Coleman, P., Howlett, L., Wheeler, P., 2003. Environmental and Health Risks Associated with the Use of Processed Incinerator Bottom Ash in Road Construction. BREWEB, Watford. www.breweb.org.uk.

Acero, J.L., Benitez, F.J., Leal, A.I., Real, F.J., Teva, F., 2010. Membrane filtration technologies applied to municipal secondary effluents for potential reuse. J. Hazard. Mater. 177, 390–398.

Amy, G., Drewes, J., 2007. Soil aquifer treatment (SAT) as natural and sustainable wastewater reclamation/reuse technology: fate of wastewater effluent organic matter (EfOM) and trace compounds. Environ. Monit. Assess. 129 (1–3), 19–26.

Azwa, Z.N., Yousif, B.F., Manalo, A.C., Karunasena, W., 2013. A review on the degradability of polymeric composites based on natural fibres. Mater. Des. 47, 424–442.

Bakopoulou, S., Emmanouil, C., Kungolos, A., 2011. Assessment of wastewater effluent quality in Thessaly region, Greece, for determining its irrigation reuse potential. Ecotoxicol. Environ. Safe 74, 188–194.

Bu, L., Wang, K., Zhao, Q.L., Wei, L.L., Zhang, J., Yan, J.C., 2010. Characterization of dissolved organic matter during landfill leachate treatment by sequencing batch reactor, aeration corrosive cell-Fenton, and granular activated carbon in series. J. Hazard. Mater. 179, 1096–1105.

Cha, W., Kim, J., Choi, H., 2006. Evaluation of steel slag for organic and inorganic removals in soil aquifer treatment. Water Res. 40, 1034–1042.

Chen, W., Westerhoff, P., Leenheer, J.A., Booksh, K., 2003. Fluorescence excitation-emission matrix regional integration to quantify spectra for dissolved organic matter. Environ. Sci. Technol. 37, 5701–5710.

Dawadi, S., Ahmad, S., 2013. Evaluating the impact of demand-side management on water resources under changing climatic conditions and increasing population. J. Environ. Manag. 114, 261–275.

Dimitrova, S.V., 2002. Use of granular slag columns for lead removal. Water Res. 36, 4001–4008.

Drewes, J.E., Reinhard, M., Fox, P., 2003. Comparing microfiltration-reverse osmosis and soil-aquifer treatment for indirect potable reuse of water. Water Res. 37, 3612–3621.

Fox, P., Aboshanp, W., Alsamadi, B., 2005. Analysis of soils to demonstrate sustained organic carbon removal during soil aquifer treatment. J. Environ. Qual. 34, 156–163.

Francois, D., 2001. Retour dèxpérience en construction routière: évaluation du comportement environnemental et mécanique de MIOM dans des chaussées sous traffic. In: Quel avenir pour les MIOM, Orléans, pp. 48–53.

Genc, A., Oguz, A., 2010. Sorption of acid dyes from aqueous solution by using non-ground ash and slag. Desalination 264, 78–83.

Geyikci, F., Kılıc, E., Coruh, S., Elevli, S., 2012. Modelling of lead adsorption from industrial sludge leachate on red mud by using RSM and ANN. Chem. Eng. J. 183, 53–59.

Gupta, V.K., Suhas, 2009. Application of low-cost adsorbents for dye removal – a review. J. Environ. Manag. 90, 2313–2342.

Hubner, U., Seiwert, B., Reemtsma, T., Jekel, M., 2014. Ozonation products of carbamazepine and their removal from secondary effluents by soil aquifer treatment–indications from column experiments. Water Res. 49, 34–43.

Komnitsas, K., Zaharaki, D., Bartzas, G., 2013. Effect of sulphate and nitrate anions on heavy metal immobilisation in ferronickel slag geopolymers. Appl. Clay Sci. 73, 103–109.

Kostura, B., Kulveitova, H., Lesko, J., 2005. Blast furnace slags as sorbents of phosphate from water solutions. Water Res. 39, 1795–1802.

Li, Y.H., Li, H.B., Sun, T.H., Wang, X., 2011. Study on nitrogen removal enhanced by shunt distributing wastewater in a constructed subsurface infiltration system under intermittent operation mode. J. Hazard. Mater. 189, 336–341.

Lin, M.Q., Ning, X.A., Liang, X., Wei, P.T., Wang, Y.J., Liu, J.Y., 2014. Study of the heavy metals residual in the incineration slag of textile dyeing sludge. J. Taiwan Inst. Chem. Eng 45, 1814–1820.

Liu, S.Y., Gao, J., Yang, Y.J., Yang, Y.C., Ye, Z.X., 2010. Adsorption intrinsic kinetics and isotherms of lead ions on steel slag. J. Hazard. Mater. 173, 558–562.

McDowell, R.W., Hawke, M., McIntosh, J.J., 2007. Assessment of a technique to remove phosphorous from streamflow. New. Zeal. J. Agric. Res. 50, 503–510.

McDowell, W.H., Zsolnay, A., Aitkenhead-Peterson, J.A., Gregorich, E.G., Jones, D.L., Jödemanne, D., Kalbitzf, K., Marschnere, B., Schwesigf, D., 2006. A comparison of methods to determine the biodegradable dissolved organic carbon from different terrestrial sources. Soil Biol. Biochem. 38, 1933–1942.

Nemati, K., Bakar, N.K.A., Abas, M.R., Sobhanzadeh, E., 2011. Speciation of heavy metals by modified BCR sequential extraction procedure in different depths of sediments from Sungai Buloh, Selangor, Malaysia. J. Hazard. Mater. 192, 402–410.

Nijhawan, A., Labhasetwar, P., Jain, P., Rahate, M., 2013. Public consultation on artificial aquifer recharge using treated municipal wastewater. Resour. Conserv. Recycling 70, 20–24.

Ortiz, N., Pires, M.A.F., Bressiani, J.C., 2001. Use of steel converter slag as nickel adsoeber to wastewater treatment. Waste Manag. 21, 631–635.

Pratt, C., Shilton, A.N., Pratt, S., Haverkamp, R.G., Bolan, N.S., 2007. Phosphorus removal mechanisms in active slag filters treating waste stabilisation pond effluent. Environ. Sci. Technol. 41, 3296–3301.

Quanrud, D.M., Arnold, R.G., Wilson, L.G., Gordon, H.J., Graham, D.M., Amy, G.L., 1996. Fate of organics during column studies of soil aquifer treatment. J. Environ. Eng. (ASCE) 122 (4), 314–321.

Quanrud, D.M., Hafer, J., Karpiscak, M.M., Zhang, H.M., Lansey, K.E., Arnold, R.G., 2003. Fate of organics during soil-aquifer treatment: sustainability of removals in the field. Water Res. 37 (14), 3401–3411.

Quanrud, D.M., Karpiscak, M.M., Lansey, K.E., Arnold, R.G., 2004. Transformation of effluent organic matter during subsurface wetland treatment in the Sonoran desert. Chemosphere 54, 777–788.

Rio, S., Verwilghen, C., Ramaroson, J., Nzihou, A., Sharrock, P., 2007. Heavy metal vaporization and abatement during thermal treatment of modified wastes. J. Hazard. Mater. 148, 521–528.

Schreiber, B., Brinkmann, T., Schmalz, V., Worch, E., 2005. Adsorption of dissolved organic matter onto activated carbon-the influence of temperature, absorption wavelength, and molecular size. Water Res. 39, 3449–3456.

Sobhani, R., McVicker, R., Spangenberg, C., Rosso, D., 2012. Process analysis and economics of drinking water production from coastal aquifers containing

chromophoric dissolved organic matter and bromide using nanofiltration and ozonation. J. Environ. Manag. 93, 209–217.
Tessier, A., Campell, P.G.C., Bisson, M., 1979. Sequential extraction procedure for the speciation of particulate trace metals. Anal. Chem. 51, 844–851.
Tiruta-Barna, L., Benetto, E., Perrodin, Y., 2007. Environmental impact and risk assessment of mineral wastes reuse strategies: review and critical analysis of approaches and applications. Resour. Conserv. Recycling 50, 351–379.
Verlicchi, P., Galletti, A., Masotti, L., 2009. A promising practice to reclaim treated wastewater for reuse: chemical disinfection followed by natural systems. Desalination 247, 490–508.
Wei, L.L., Wang, K., Zhao, Q.L., Xue, S., Jia, T., You, P.Y., 2010. Evaluation of fly-ash additive for removal of dissolved organic matter during soil aquifer treatment of WWTP effluent. J. Chem. Technol. Biotechnol. 85, 1445–1454.
Wei, L.L., Zhao, Q.L., Xue, S., Chang, C.C., Tang, F., Liang, G.L., Jia, T., 2009a. Reduction of trihalomethane precursors of dissolved organic matter in the secondary effluent by advanced treatment processes. J. Hazard. Mater. 169, 1012–1021.
Wei, L.L., Zhao, Q.L., Xue, S., Jia, T., Tang, F., You, P.Y., 2009b. Behavior and characteristics of DOM during a laboratory-scale horizontal subsurface flow wetland treatment: effect of DOM derived from leaves and roots. Ecol. Eng 35, 1405–1414.
Westerhoff, P., Pinney, M., 2000. Dissolved organic carbon transformations during laboratory scale groundwater recharge using lagoon-treated wastewater. Waste Manag. 20 (13), 75–83.
Xue, S., Zhao, Q.L., Wei, L.L., Wang, L.N., Liu, Z.G., 2007. Fate of secondary effluent dissolved organic matter during soil-aquifer treatment. Chin. Sci. Bull. 52 (18), 2496–2505.
Xue, S., Zhao, Q.L., Wei, L.L., Jia, T., 2008. Trihalomethane formation potential of organic fractions in secondary effluent. J. Environ. Sci. Chin. 20, 520–527.
Xue, S., Zhao, Q.L., Wei, L.L., Ren, N.Q., 2009a. Behavior and characteristics of dissolved organic matter during column studies of soil aquifer treatment. Water Res. 43, 499–507.
Xue, Y.J., Hou, H.B., Zhu, S.J., 2009b. Adsorption removal of reactive dyes from aqueous solution by modified basic oxygen furnace slag: isotherm and kinetic study. Chem. Eng. J. 147, 272–279.
Yang, X., Shang, C., Lee, W.T., Westerhoff, P., Fan, C.H., 2008. Correlations between organic matter properties and DBP formation during chloramination. Water Res. 42, 2329–2339.
Zhang, Q.H., Wang, X.C., Xiong, J.Q., Chen, R., Cao, B., 2010. Application of life cycle assessment for an evaluation of wastewater treatment and reuse project–Case study of Xi'an, China. Bioresour. Technol. 101, 1421–1425.
Zhou, Y., Ning, X.A., Liao, X.K., Lin, M.Q., Liu, J.Y., Wang, J.H., 2013. Characterization and environmental risk assessment of heavy metals found in fly ashes from waste filter bags obtained from a Chinese steel plant. Ecotoxicol. Environ. Saf. 95, 130–136.